J Nanopart Res (2010) 12:2037–2044
DOI 10.1007/s11051-009-9760-5

RESEARCH PAPER

Interparticle forces in silica nanoparticle agglomerates

M. Seipenbusch · S. Rothenbacher · M. Kirchhoff · H.-J. Schmid · G. Kasper · A. P. Weber

Received: 2 June 2008 / Accepted: 3 September 2008 / Published online: 27 September 2009

Abstract To improve the understanding of the poor dispersability of fumed silica nanoparticle agglomerates, the stability of highly defined agglomerated model particles was investigated. The high temperature synthesis conditions for fumed silica were simulated by tempering. Along with electron-microscopical analysis of the sintering necks, the interparticle forces were investigated by energy resolved fragmentation analysis based on low pressure impaction. At temperatures above 1,000 °C the fragmentability of the agglomerates rapidly decreased while the energy necessary for fragmentation increased. The development of sintering necks was observed for temperatures exceeding 1,300 °C. Comparison of the experimental data with the fragmentation behaviour of a commercially produced fumed silica indicated solid state contacts (sintering necks) as being most numerous in the agglomerates resulting in limited fragmentability.

Keywords Fragmentation · Sintering · Van-der-Waals forces · Agglomerate stability · Nanoscale interactions

M. Seipenbusch (✉) · S. Rothenbacher · G. Kasper
Institut für Mechanische Verfahrenstechnik und Mechanik, Universität Karlsruhe (TH), Am Forum 8, 76131 Karlsruhe, Germany
e-mail: martin.seipenbusch@kit.edu

M. Kirchhoff
Lehrstuhl für Feststoff- und Grenzflächenverfahrenstechnik, Friedrich-Alexander-Universität Erlangen-Nürnberg, Cauerstraße 4, 91058 Erlangen, Germany

H.-J. Schmid
Mechanische Verfahrenstechnik und Umweltverfahrenstechnik, Universität Paderborn, Pohlweg 55, 33098 Paderborn, Germany

A. P. Weber
Institut für Mechanische Verfahrenstechnik, Technische Universität Clausthal, Leibnizstrasse 19, 38678 Clausthal-Zellerfeld, Germany

Introduction

In the synthesis of nanoparticles (NP) the high number concentrations, unavoidable in an even moderate yield process, lead to the formation of agglomerates. This is especially true in the aerosol phase, where stabilization of particles in the unagglomerated state is quite challenging. Upon contact the primary particles of an agglomerate form bonds which can be of different nature, depending on the synthesis process. At sufficiently high temperatures for instance, the viscosity of the particles or the diffusivity allow sintering of the particles in contact, and thus hard aggregates are formed. Depending on the chemical nature of the particles, the formation of chemical bonds between the particle surfaces may also occur. As a baseline of the interparticle energy van der Waals

forces are always present, leading to relatively weak agglomerates. If condensable material is present in the surrounding atmosphere, the formation of liquid bridges can be an additional contribution.

While aggregates are very stable structures that can hardly be broken up, agglomerates can be disintegrated in suitable processes for further use. The distinction between agglomerates and aggregates is significant to estimate the product properties of nanopowders since the strength of interparticle bonds to a large extent determines the physical properties and applicability in subsequent manufacturing steps. On one hand, there are nanomaterials that have to be applied in single particle form, e.g., in electronic, optical, and optoelectronic applications. In these cases, the energy needed for particle deagglomeration is an important parameter. This is also true for the fluidization of agglomerated NP where the size of the stabile macro agglomerates formed in the fluidized bed results from an equilibrium between attractive interparticle forces and disruptive influences originating from shear and impact forces (Wang et al. 2002; Valverde and Castellanos 2008). In filled polymers, however, the elasticity of nanoparticle chain aggregates seems to contribute to the mechanical properties of the composite material, thus the strength of the interparticle forces is of importance in a positive way (Bandyopadhyaya et al. 2004). In biological systems the strength of NP agglomerates has yet another implication. Since both the uptake of particles by cells and the toxic effect appear to be dependent on particle size (Rejman et al. 2004; Oberdörster et al. 1992) the integrity of agglomerates is crucial in respect to health hazard assessment of NP.

As a major representative of engineered NP, the agglomerate strength of fumed silica deserves special attention. For this material a limit of the dispersibility in liquid media and polymers is observed. In liquids the particles remain at diameters of about 100 nm, while the primary particles are much smaller than this, in the range of 10–20 nm. An increase of the energy input does not lead to further fragmentation (e.g., Pohl et al. 2005; Wengeler et al. 2006). While electron micrographs show no signs of sintering there are obviously substructures of the agglomerates with high interparticle forces that cannot be fragmented. In polymers the dispersion of flame made SiO_2 agglomerates was found to be equally challenging and complete deagglomeration was not achieved (Bikiaris et al. 2005). It can be speculated that these stabile substructures are aggregates, formed in regions of high temperature in the synthesis process where minute sintering in the contact regions was possible. These aggregates may then agglomerate in cooler regions to form weak agglomerates.

The aim of this study was the systematic investigation of the interparticle forces in silica agglomerates. To this end silica particles were generated and allowed to agglomerate at room temperature, forming low energy contacts. The formation of high energy bonds was then induced by controlled sintering at various temperatures between 1,000 and 1,500 °C at a constant residence time of 30 ms. The bond energies of the primary particles within the agglomerates were determined using the method of impact fragmentation, which was adapted to the nanoscale (Seipenbusch et al. 2002, 2007). The method enables fragmentation of agglomerates under variation of the kinetic energy prior to impaction. Analysis of the fragmentation patterns at different initial kinetic energies then yields fragmentation curves that show the distribution of interparticle forces within the agglomerates. In parallel to the fragmentation experiments the evolution of solid state bridges was analysed using electron microscopy.

Experimental

The experimental setup combined particle synthesis, sintering step and the analysis of the interparticle forces into a direct line, without any intermediate deposition (Fig. 1). Thus, the effect of high temperature on the strength of the agglomerates was analysed quasi in situ. Spherical particles were generated at high temperatures which were then agglomerated at

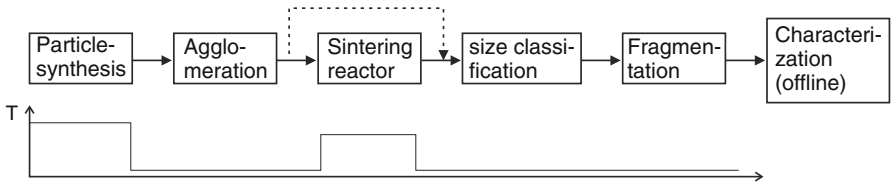

Fig. 1 Schematic of the experimental setup

room temperature. After the passage of the sintering reactor a narrow size fraction with a median diameter of 300 nm was classified in a differential mobility analyzer (DMA, TSI model 3010). Subsequently, the aerosol entered the device for fragmentation analysis. The individual parts of the setup will be discussed in more detail in the following.

Particle generation

In a hot wall tubular reactor single spherical silica nanoparticles were produced by oxidation of the precursor tetraethylorthosilicate (TEOS). These particles served as monomers for silica agglomerates. To generate particles for fragmentation analysis the synthesis reactor was run at a temperature of 1,750 °C at a pressure of 950 mbar. For these conditions a residence time of 0.8 s and silica mass concentration of 0.6 g/m^3 were determined. An aerosol with a relatively narrow size distribution ($\sigma_g = 1.35$) and a median size of 25 nm was obtained in this way (see Fig. 2). Coagulation at room temperature led to the formation of agglomerates consisting of approx. 100 primary particles. These larger agglomerates simplify statistical evaluation of the fragmentation experiments.

The analysis of neck formation during sintering in the TEM, however, required highly defined doublets of particles with narrow size distributions. For this purpose the particle synthesis reactor was adjusted in two ways. First, at the end of the reactor an additional quench probe was applied to reduce the concentration. Second, residence time and mass concentration were set to 0.9 s and 0.5 g/m^3, respectively. The other parameters were identical to the ones used in the fragmentation experiments. Further details on the particle synthesis may be found elsewhere (Kirchhof et al. 2004).

For well-defined sintering and investigation of the sintering kinetics separate from other mechanisms possibly occurring in a subsequent reactor, the synthesis parameters ensured complete oxidation of the precursor in the synthesis reactor. Otherwise particle formation due to nucleation and surface growth may also occur in the sintering reactor.

After passing a cold coagulation zone the silica agglomerates enter a specifically designed high-temperature, short-time sintering reactor (Kirchhof et al. 2009). The reactor allows gas temperatures of up to 1,600 °C and well-defined residence times down to 4 ms in the reaction zone. For the experiments temperatures in the range of 1,000–1,500 °C were used while the residence time of 30 ms was kept constant. The process pressure was set to 600 mbar. A schematic drawing of the short-time sintering reactor is shown in Fig. 3. The reactor consists of an outer alumina made ceramic tube and an inner ceramic setup, housed within an electrical furnace, all vertically positioned.

The preheated process air enters the reactor at the bottom and is further heated to sintering temperature between the outer ceramic tube and the inner ceramic setup assisted by several axial heat transfer ceramic plates. The sintering zone with a length of 400 mm is located in the inner setup between water-cooled injection and collection probes. This way, rapid heating and cooling of the particles at the beginning and at the end of the sintering zone, respectively, is maintained. More specifically, the heating of the small cold aerosol flow is achieved by mixing with the hot process air when entering the reaction zone after the injection probe. The collection probe delivers quench air to the aerosol flow to reduce the temperature by several hundred degrees at the end of the sintering zone. Thus, an almost instantaneous quenching of the sintering processes is achieved. Both water-cooled probes are embedded in

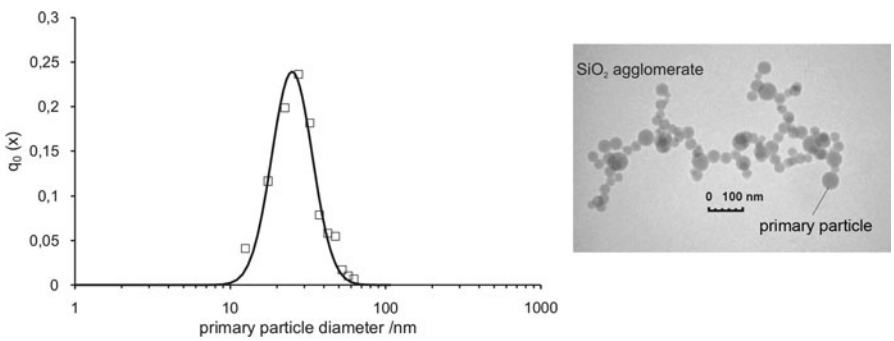

Fig. 2 *Left hand side*: primary particle size distribution of silica agglomerates used in the fragmentation experiments. *Right hand side*: SiO_2 agglomerate, as produced

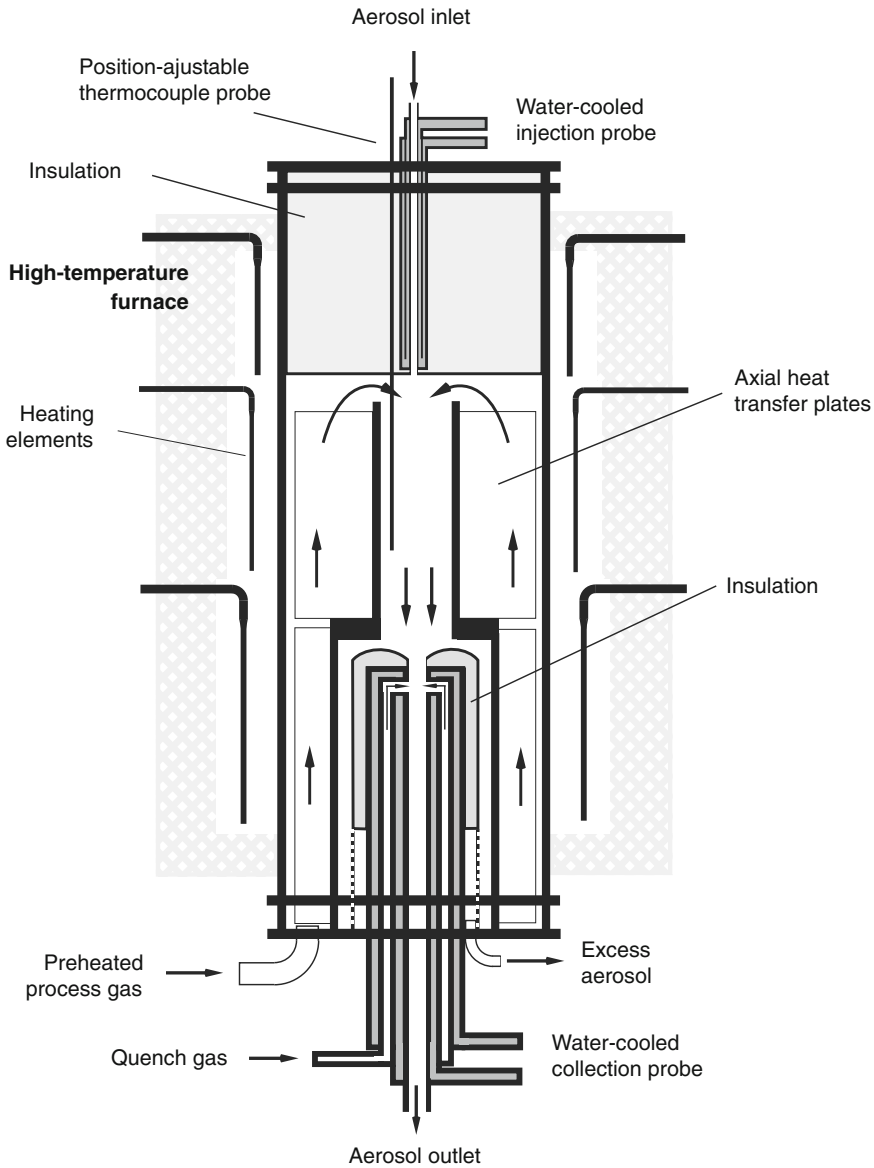

Fig. 3 Schematic of the sintering reactor

alumina–silica made fibre insulation to minimise heat transfer from the sintering zone. In order to minimise near wall effects only part of the sintered aerosol flow exits through the line of the water-cooled collection probe and is used for analysis. The excess aerosol flow exits beneath the probe and is not used.

Analysis of agglomerate strength by impact fragmentation

The experimental system for impact fragmentation was described earlier in detail (Seipenbusch et al. 2002), thus only a brief outline will be given here. The core of the setup is a single stage low pressure impactor (LPI). An aerosol flow passes through a critical orifice, which defines the mass flow to the impactor. An acceleration nozzle then focuses the aerosol onto the impaction plate perpendicular to the flow, where a sharp directional change of the flow occurs (see Fig. 4). Due to their inertia particles are unable to follow the gas flow and are deposited on the impaction plate. The particle surface concentration was kept low enough to prevent re-agglomeration of impacted particles on the plate. The pressure downstream of the critical orifice determines the velocity

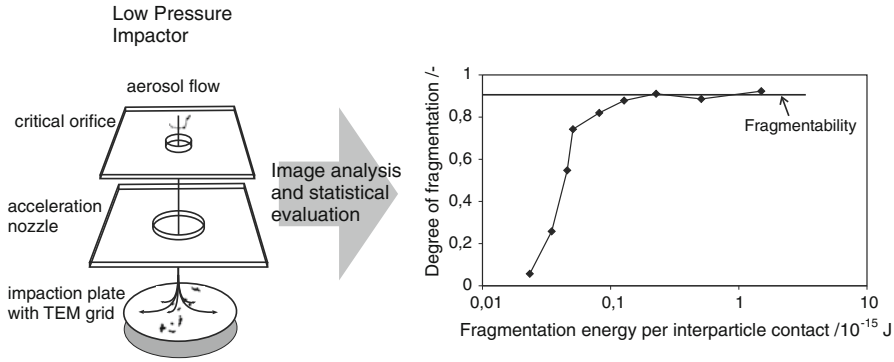

Fig. 4 Schematic of the experimental method for energy resolved fragmentation analysis and exemplary fragmentation curve (SiO_2 as produced)

of the gas and thus the kinetic energy of an impacting particle. Variation of the pressure in the LPI thus allows the variation of the energy available for fragmentation of an impacting agglomerate. The impaction plate is equipped with a filmed TEM-grid. Samples of the aerosol are first collected by diffusion, to define the original state of agglomeration. For this, the number of primary particles and the number of interparticle bonds is determined from TEM images. Subsequently, the pressure in the LPI is lowered in steps and sampling of impacted particles is performed at each pressure. The fragmentation patterns are now analysed in the same way as the intact agglomerates. A statistical analysis is then carried out yielding a fragmentation curve as displayed in Fig. 4 for agglomerated Ni nanoparticles. We define agglomerate fragmentation in the following manner (Eq. 1):

$$F = 1 - \frac{\#c}{\#pp} \Big/ \left(\frac{\#c}{\#pp}\right)_0 = 1 - \frac{c_N}{c_{N,0}} \qquad (1)$$

The number of contacts within an agglomerate ($\#c$) is compared to the number of primary particles ($\#pp$) and is divided by the initial ratio of the same numbers for the intact agglomerate. This is equivalent to a comparison of the coordination number c_N before and after fragmentation.

The fragmentation curves can reveal several agglomerate characteristics. By fitting a normal distribution to the data a value of the kinetic energy necessary to achieve 50% fragmentation ($E_{\mathrm{kin},50\%}$) and the width of the distribution (σ_g) can be obtained, which are very valuable parameters to describe the overall fragmentation behaviour. We define the maximum of the fragmentation curves in the observed energy range as the *Fragmentability* f of an agglomerate. It is a direct measure for the fraction of breakable contacts to more rigid interparticle bonds. Thus, it can be used to distinguish between agglomerates and aggregates.

Results and discussion

The mechanical properties of Aerosil® 200 (Degussa), as a reference material for an industrially produced fumed silica, were analysed by impact fragmentation. The median primary particle size of 25 nm was determined by image analysis (see Fig. 5, left). The fragmentation experiments yielded a value for $E_{\mathrm{kin},50\%}$ of 5.5×10^{-17} J/particle and a fragmentability of about 30% (see Fig. 5 right). This

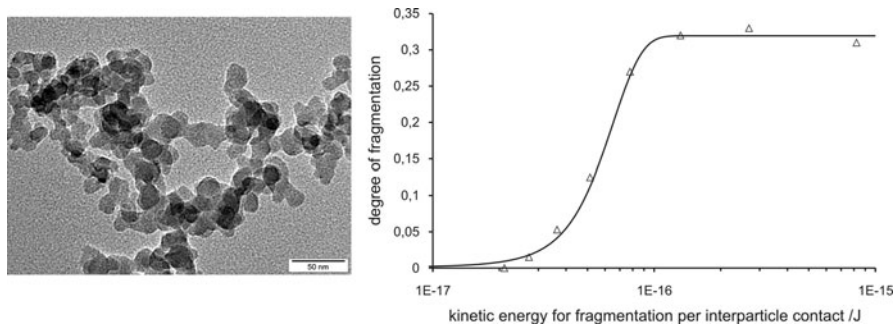

Fig. 5 TEM image of agglomerate/aggregate of Aerosil® 200 and fragmentation curve of the same material

result supports the observations of limited dispersability of fumed silica in the liquid phase.

A simulation of the particle synthesis was now done using the techniques for monomer synthesis and sintering under highly controlled conditions, as described above. The stability of the SiO_2 agglomerates was investigated for the as produced state and for six temperature settings of the sintering reactor between 1,000 and 1,500 °C using the low pressure impactor. The results are displayed in Fig. 6 where the lines represent lognormal distributions fitted to the data. Since the fragmentation curves can be viewed as representing the distribution of bond energies between the primary particles of an agglomerate, the changes in these curves during the sintering process contain valuable information. The maximum reached in the observed energy range, the fragmentability f, decreases substantially with increasing temperature. Since the kinetic energies applied for fragmentation are too low to break solid state sintering bonds but sufficient to break weaker contacts as van der Waals and liquid bridge bonds, f is equivalent to the fraction of soft interparticle bonds. Thus, for the highest temperatures we have almost pure aggregates, while the as produced particles are agglomerates held together by van der Waals forces and liquid bridge bonds alone. The right shift of the curves indicates an increase of the average bond energy in the breakable bonds.

For better interpretation of the fragmentation data the sintering of doublets of equally sized SiO_2 particles was investigated in the same setup. As a measure for the sintering progress, the sintering neck

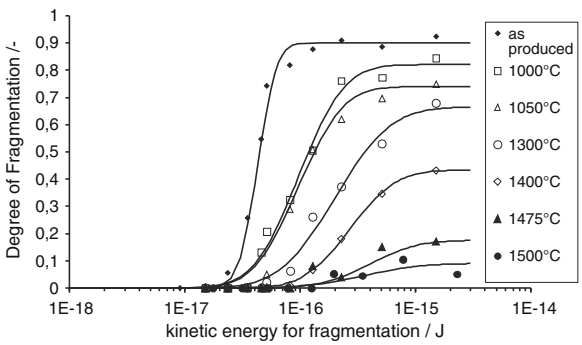

Fig. 6 Some of the fragmentation curves determined by impact fragmentation for as produced agglomerates of SiO_2 and after various stages of sintering at a constant residence time of 30 ms

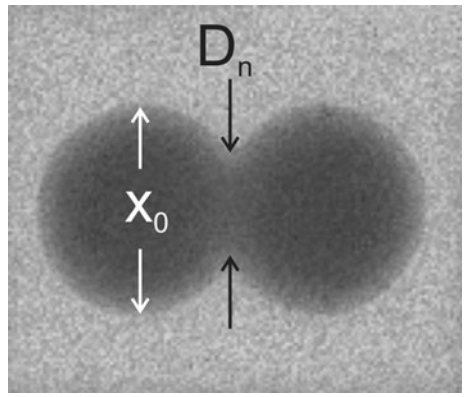

Fig. 7 Sintering neck diameter (D_n) evaluation by TEM-analysis of SiO_2 doublets with primary particle size x_0

size was determined by offline analysis in the TEM. Figure 7 exemplarily shows the TEM-analysis for neck size evaluation.

The dimensionless sintering neck diameter D_n/x_0 is determined by the quotient of the neck diameter D_n and the primary particle diameter x_0. For small neck diameters the size of the neck region in the direction of the symmetry axis of the initially spherical primary particles is very small and consequently, the minimum neck size that can be clearly determined and evaluated by TEM-analysis is in the range of $D_n/x_0 = 0.2$–0.3. Figure 8 shows D_n/x_0 as a function of the temperature for different particle sizes x_0 and for a constant residence time of 28 ms. Complete sintering was achieved when D_n/x_0 reached unity, which was only accomplished for the smallest particle size.

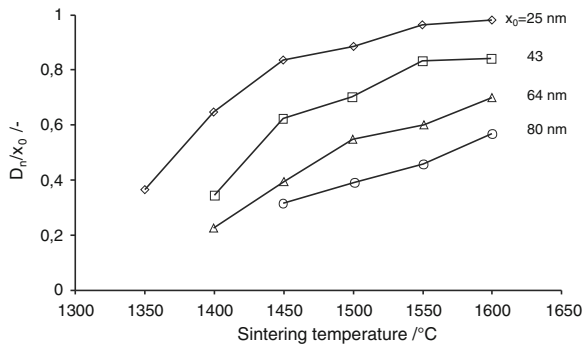

Fig. 8 Sintering neck size D_n/x_0 of silica nanoparticle doublets for different temperatures and a constant residence time of $t = 28$ ms

Since the sintering experiments described here were conducted with single particle contacts between particles of sizes predefined in the synthesis reactor the sintering progress can be resolved depending on the primary particle size. A dependence of the relative neck diameter on both temperature and primary particle size is clearly visible in the diagram, where the elevation of the first and the reduction of the latter substantially increase the sintering neck size. A detailed investigation of the sintering kinetics of silica doublets depending on particle size, temperature, and residence time are described elsewhere (Kirchhof et al. 2009).

To compare the two sets of data the parameters describing the fragmentation were derived from the fit curves to the data. The width of the distributions (σ_g from the log-normal distributions) increased from an initial value of 1.35 to values that scattered around 2. The fact that the initial σ_g equals the value of the primary particle size distribution is very interesting. If it is assumed that coagulation occurs statistically between all particle sizes in agglomerate formation there is a distribution of the size dependent interparticle forces. For van der Waals forces and liquid bridge bonds the interparticle energy is proportional to the particle size. We thus see an indication for these two forces to be the dominant interparticle forces between the particles in the agreement of the values for σ_g. The increase of σ_g with the sintering temperature for the energy distribution is not parallelled by an equal broadening of the primary particle size distribution and could be due to an additional interparticle force like chemical bonds between the particles that may be formed below the sintering level.

The fragmentability and the kinetic energy for 50% fragmentation were also derived and are plotted in Fig. 9. For comparison the relative neck diameter is plotted over the sintering temperature for the doublets with x_0 equalling the median diameter of the agglomerate primary particle size distribution. The energy needed for the breakage of the fraction of breakable bonds given by f increases significantly for temperatures exceeding 1,000 °C while in the range from 25 °C to this temperature no change was observed. For temperatures exceeding 1,350 °C sintering eventually becomes apparent in the development of solid state necks and complete sintering is achieved at 1,550 °C. In the same temperature regime

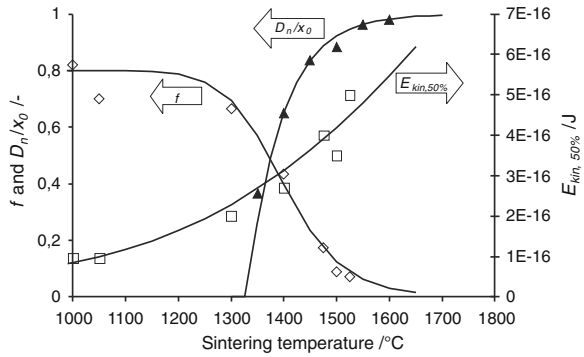

Fig. 9 Parameters describing the fragmentation energy distribution, the fragmentability f and the median kinetic energy for the fracture of 50% of the interparticle bonds and the relative neck diameter of the particles during sintering for doublets with $x_0 = 25$ nm. The lines are merely guides for the eye

the fragmentability drops to values close to zero and $E_{kin,50\%}$ rises to roughly twice the plateau value.

Since the primary particles of the agglomerates are not uniform in size there is also a distribution of the progress of neck formation. As Fig. 8 shows, there is a strong particle size dependence of the sintering kinetics, which will lead to some very rigid bonds between smaller particles in an agglomerate while larger ones will still be held together by van der Waals bonds or liquid bridges. Thus, the emergence of the first sintering bonds will reduce the fragmentability but will not transform the agglomerate entirely into an aggregate.

Conclusions

The experiments with our synthesized SiO_2 showed, that particles agglomerated at room temperature are indeed held together by relatively weak forces and can be deagglomerated almost entirely. At temperatures higher than 1,000 °C, however, the maximum degree of deagglomeration (fragmentability) obtainable in the applied energy range rapidly decreased. When sintering necks eventually became visible at temperatures above 1,300 °C the fragmentability had already dropped to about 50%. The fragmentation curve of Aerosil® 200 was approximated for temperatures exceeding 1,400 °C. The interparticle contacts in fumed silica therefore appear to be dominated by solid state necks. The implication of this for the dispersability is already known. It is possible to break the van

der Waals contacts and liquid bridges between the aggregates but under application of energies within an economically reasonable range it is impossible to break the aggregates, thus a fragmentation down to the primary particle size cannot be achieved.

For the fluidization of NP at high temperatures, e.g., in a catalytic reactor, the increase in interparticle forces observed may lead to an increase in the size of stabile agglomerates and thus to a change in fluidization behaviour. From the point of view of NP toxicology, the implication of the experimental results is that the size of the aggregates rather than the size of the primary particles is a relevant metric for mechanisms depending on particle geometry such as transport and cell uptake, determining the fate of a particle in an organism.

Acknowledgments The authors express their gratitude for the funding of this project by the Deutsche Forschungsgemeinschaft under grant number KA 1373.

References

Bandyopadhyaya R, Rong W, Friedlander SK (2004) Dynamics of chain aggregates of carbon nanoparticles in isolation and in polymer films: Implications for nanocomposite materials. Chem Mater 16:3147–3154

Bikiaris DN, Papageorgiou GZ, Pavlidou E, Vouroutzis N, Palatzoglou P, Karayannidis GP (2005) Preparation by melt mixing and characterization of isotactic polypropylene/SiO2 nanocomposites containing untreated and surface-treated nanoparticles. J Appl Polym Sci 100:2684–2696

Kirchhof MJ, Schmid H-J, Peukert W (2004) Reactor system for the study of high-temperature short-time sintering of nanoparticles. Rev Sci Instrum 75:4833–4840

Kirchhof MJ, Schmid H-J, Peukert W (2009) (in preparation)

Oberdörster G, Ferin J, Gelein R, Soderholm SC, Finkelstein J (1992) Role of the alveolar macrophage in lung injury: studies with ultrafine particles. Environ Health Perspect 97:193–199

Pohl M, Schubert H, Schuchmann HP (2005) Herstellung stabiler Dispersionen aus pyrogener Kieselsäure. Chem Ing Tech 77:258–262

Rejman J, Oberle V, Zuhorn IS, Hoekstra D (2004) Size-dependent internalization of particles via the clathrin- and caveolae-mediated endocytosis. Biochem J 377:159–169

Seipenbusch M, Froeschke S, Weber AP, Kasper G (2002) Investigations on the fracturing of nanoparticle agglomerates—first results. J Proc Mech Eng 216:219–225

Seipenbusch M, Toneva P, Peukert W, Weber AP (2007) Impact fragmentation of metal nanoparticle agglomerates. Part Part Syst Charact 24:193–200

Valverde JM, Castellanos A (2008) Fluidization of nanoparticles: a simple equation for estimating the size of agglomerates. Chem Eng J 140:296–304

Wang Y, Gu G, Wei F, Wu J (2002) Fluidization and agglomerate structure of SiO_2 nanoparticles. Powder Technol 124:152–159

Wengeler R, Teleki A, Vetter M, Pratsinis SE, Nirschl H (2006) High-pressure liquid dispersion and fragmentation of flame-made silica agglomerates. Langmuir 22:4928–4935